Phys. Lett. B 860 (2025) 139175

Contents lists available at ScienceDirect

Physics Letters B

journal homepage: www.elsevier.com/locate/physletb

Letter

A study of the ϕN correlation function

Luciano M. Abreu [a], Philipp Gubler [b,d], K.P. Khemchandani [c], A. Martínez Torres [d,*], Atsushi Hosaka [b,d,e]

[a] Instituto de Física, Universidade Federal da Bahia, 40210-340, Salvador, BA, Brazil
[b] Advanced Science Research Center, Japan Atomic Energy Agency, Tokai, Ibaraki 319-1195, Japan
[c] Universidade Federal de São Paulo, C.P. 01302-907, São Paulo, Brazil
[d] Universidade de Sao Paulo, Instituto de Fisica, C.P. 05389-970, São Paulo, Brazil
[e] Research Center for Nuclear Physics (RCNP), Osaka University, Ibaraki 567-0047, Japan

ARTICLE INFO

Editor: H. Gao

ABSTRACT

The femtoscopic ϕN correlation function is studied within a hadronic effective Lagrangian approach with coupled channels, based on hidden local symmetry. The results are compared with the data recently reported by the ALICE collaboration. We find that the correlation function has very different features for the ϕN system in the spin 1/2 and 3/2 configurations, with the spin-averaged combination matching well with the experimental data. A strong attraction, leading to the formation of a ϕN bound state or a very prominent cusp is found in the spin 3/2 case. The correlation function for spin 1/2, on the other hand, is strongly impacted by the negative parity $N^*(1895)$ nucleon resonance.

1. Introduction

A first näive guess on the nature of the ϕ-N interaction could be biased by the Okubo-Zweig-Iizuka (OZI) rule which would imply a weak interaction among the two hadrons due to their distinct quark contents. A more careful line of reasoning would, however, already raise questions on possible coupled channel effects. Indeed, the experimental study of correlations of $p-\phi \oplus \bar{p}-\phi$ pairs, measured in high-multiplicity pp collisions at $\sqrt{s} = 13$ TeV by the ALICE Collaboration [1], indicates that the relevant interactions are far from those expected by the OZI suppression. A Lednický–Lyuboshits fit to the data led to a spin-averaged scattering length of $(0.85 \pm 0.34 \pm 0.14) + i\,(0.16 \pm 0.1 \pm 0.09)$ fm, which was interpreted as an attractive interaction. Soon after the publication of Ref. [1], another piece of useful information on the ϕN interaction was obtained from lattice QCD simulations based on the HAL QCD method [2]. Specifically, Ref. [2] reported values of the scattering length and the effective range for the ϕN interaction in the spin-3/2 configuration as $a^{(3/2)} = -1.43(23)^{+36}_{-06}$ fm and $r_{\rm eff}^{(3/2)} = 2.36(10)^{+02}_{-48}$ fm, showing that the interaction is attractive. All these results seem to be at odds with the one inferred from the ϕ photoproduction data [3], which implies a weak ϕN interaction as would be expected from the OZI rule. Using the findings of Refs. [1,2], a fit was made to the data on the correlation function in Ref. [4] by constraining the spin 3/2 interaction using the scattering length determined by lattice QCD simulations [2]. As a result, evidence for a ϕN bound state was found for the spin 1/2 channel. Yet another fit to the same data was recently presented in Ref. [5], in which the correlation function was calculated using vector meson-baryon amplitudes obtained within a coupled channel approach based on hidden local symmetry (HLS). The interactions in this model proceed through a t-channel vector-meson exchange, which leads to spin-independent correlation functions, and that differs from the findings of Ref. [4].

In this paper, we present a different approach, where we do not make a fit, but simply use the previous results of Refs. [6–8]. In Refs. [6,7], a formalism for meson-baryon interactions was developed by treating vectors and pseudoscalars on an equal footing up to all orders of the scattering equation. Besides, it was found that a contact interaction coming from the HLS Lagrangian and u-channel interactions gave contributions comparable to those coming from the t-channel diagrams. Consequently, the interactions were found to be both spin and isospin-dependent. Refs. [6,7] were further extended in Ref. [8] by constraining the model parameters to reproduce some relevant experimental data on pseudoscalar-baryon final states. It is worth mentioning that the same model has been successfully applied to the study of several meson-baryon systems, predicting observables and reproducing experimental

* Corresponding author.
E-mail addresses: luciano.abreu@ufba.br (L.M. Abreu), philipp.gubler1@gmail.com (P. Gubler), kanchan.khemchandani@unifesp.br (K.P. Khemchandani), amartine@if.usp.br (A. Martínez Torres), hosaka@rcnp.osaka-u.ac.jp (A. Hosaka).

https://doi.org/10.1016/j.physletb.2024.139175
Received 16 September 2024; Received in revised form 11 November 2024; Accepted 1 December 2024

Available online 4 December 2024

data when available [9–13]. Here, we will stay very close to the works of Refs. [6–8], where it was shown that the amplitudes resulting from the coupled channel treatment exhibit a strong attraction near the ϕN threshold in the spin 3/2 channel, while a weaker attraction is obtained in the spin 1/2 case (near the ϕN threshold). As we will show, we find that such amplitudes lead to correlation functions that are different for the two spin cases, and are more in line with the findings of Ref. [4].

The nature and strength of the ϕ-N interaction is of interest also in the context of studying in-medium behavior of the ϕ meson in nuclear matter [14–16] and the possibility of the formation of a ϕ-nucleus bound state [17–22], for which the state discussed in Ref. [4] would be the most elementary type. While the KEK E325 Collaboration reported a negative mass shift of $-3.4^{+0.6}_{-0.7}\%$ for the ϕ meson in nuclear matter [23], the values of the above recently measured scattering lengths around 1 fm translate, within the linear density approximation, to mass shifts of the order of 10% [24] (see Ref. [25] for a discussion of some of the effects that go beyond linear density). The J-PARC E16 [15] and E88 [26] experiments will hopefully shed new light on this issue by providing updated measurements of the ϕ meson mass shift in nuclear matter. This paper will tackle the problem from the opposite side, by giving an improved interpretation of the ALICE ϕN correlation function data based on a phenomenologically successful coupled channel approach, as described in the previous paragraph.

This paper is organized as follows. We start by giving a brief outline of the model we use to determine meson-baryon amplitudes and the formalism to apply those amplitudes for computing the ϕN correlation function. Finally, we present the main results of this work, the ϕN correlation function, and its comparison with the available experimental data. We furthermore provide the decomposition of the spin-averaged correlation function into different spins and channels and discuss the corresponding results. The paper concludes with a summary.

2. Formalism

2.1. Meson-baryon scattering amplitudes

In this section, we first briefly discuss the calculation of the ϕ-N amplitudes which result from solving the Bethe-Salpeter equation. For more details, we refer the reader to Refs. [6–8]. The amplitudes were obtained in these former works by considering the following meson-baryon systems to build the coupled channel space in spin 1/2: πN, ηN, $K\Lambda$, $K\Sigma$, ρN, ωN, ϕN, $K^*\Lambda$, and $K^*\Sigma$. It is important to mention that all the amplitudes are projected on the s-wave. In such a framework, only vector-baryon systems can couple to a total spin 3/2 and, thus, the number of coupled channels is reduced in this case. The lowest-order vector-baryon interactions in our formalism are determined, through the Lagrangian [6,8]

$$\mathcal{L}_{VB} = -g\Big\{\langle\bar{B}\gamma_\mu\left[V_8^\mu, B\right]\rangle + \langle\bar{B}\gamma_\mu B\rangle\langle V_8^\mu\rangle + \frac{1}{4M}\Big(F\langle\bar{B}\sigma_{\mu\nu}\left[V_8^{\mu\nu}, B\right]\rangle + D\langle\bar{B}\sigma_{\mu\nu}\left\{V_8^{\mu\nu}, B\right\}\rangle\Big) + \langle\bar{B}\gamma_\mu B\rangle\langle V_0^\mu\rangle + \frac{C_0}{4M}\langle\bar{B}\sigma_{\mu\nu}V_0^{\mu\nu}B\rangle\Big\}, \quad (1)$$

where the subscripts 8 and 0 represent the flavor octet and the singlet part of the wave function of the vector mesons. Such a separation is relevant for ω and ϕ which are considered as ideally mixed states of the octet and singlet components. The tensor field, $V^{\mu\nu}$, is written as

$$V^{\mu\nu} = \partial^\mu V^\nu - \partial^\nu V^\mu + ig\left[V^\mu, V^\nu\right], \quad (2)$$

with V^μ being the SU(3) matrix for the (physical) vector mesons

Four types of diagrams are determined from Eq. (1), which are shown in Fig. 1(A)-(D). The spin part of the amplitudes corresponding to these four diagrams turns out, in the order the diagrams are shown, to be (A) $\vec{\epsilon}_i\cdot\vec{\epsilon}_f$, (B) $\vec{\sigma}\cdot\vec{\epsilon}_f\times\vec{\epsilon}_i$, (C) $\vec{\epsilon}_i\cdot\vec{\sigma}\,\vec{\epsilon}_f\cdot\vec{\sigma}$ and (D) $\vec{\epsilon}_f\cdot\vec{\sigma}\,\vec{\epsilon}_i\cdot\vec{\sigma}$, where $\vec{\epsilon}_{i/f}$ are the polarization vectors of the participating vector meson, while $\vec{\sigma}$ operates in the bayonic spin space.

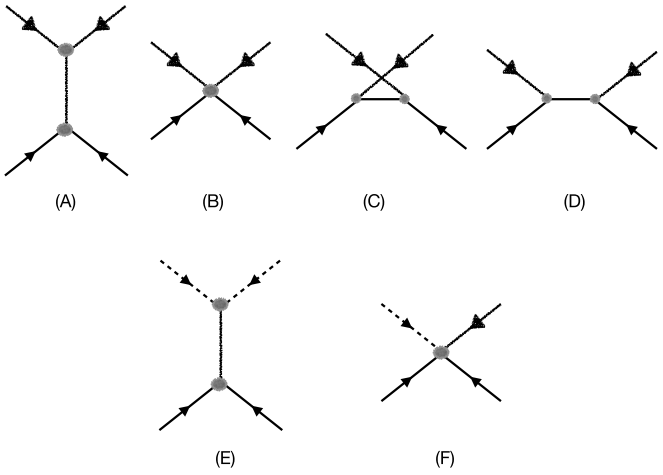

Fig. 1. The upper row of diagrams corresponds to the lowest order contributions to the vector-baryon interactions. The lower row shows the lowest-order pseudoscalar-baryon amplitude and the one for the transition between the two types of systems. We represent baryons as solid lines, vector mesons as thick-smeared lines, and pseudoscalar mesons as dashed lines.

The pseudoscalar-baryon interactions in Refs. [6–8] were determined from the lowest-order chiral Lagrangian (represented by diagram (E) in Fig. 1). The transitions among the two types of meson-baryon systems were determined by introducing vector-mesons as gauge bosons in the nonlinear sigma model Lagrangian. We can interpret such amplitudes as an extension of the Kroll-Ruddermann term for the pion-photoproduction where a photon is replaced by a vector meson, relying on the vector meson dominance.

We next discuss how these amplitudes are used as an input in the calculation of the correlation function.

2.2. Correlation function

The two-particle correlation function (CF) is formally defined as the ratio of the probability of measuring the two-particle state and the product of the probabilities of measuring each individual particle. After the use of some approximations (see a detailed discussion, for example, in Ref. [27]), it may be written in terms of the so-called Koonin–Pratt formula [27–31]

$$C(k) = \int d^3r S_{12}(\vec{r})|\Psi(\vec{k};\vec{r})|^2, \quad (3)$$

where $\vec{k}$ is the relative momentum in the center of mass (CM) frame of the pair; $\vec{r}$ is the relative distance between the two particles; $\Psi(\vec{k};\vec{r})$ is the relative two-particle wave function; and $S_{12}(\vec{r})$ is the source function.

For our practical purposes here, to accommodate the multi-channel amplitudes presented in the previous section, we use a generalized version of the Koonin–Pratt formula (3) developed in preceding works [32–35]. The same formalism has been applied recently to studies of several systems leading to the formation of exotic hadrons (for a review see Ref. [36]). Accordingly, the coupled-channel CF for a specific channel i is given by

$$C_i(k_i) = 1 + 4\pi\theta(q_{max}-k_i) \times \int_0^\infty dr r^2 S_{12}(\vec{r})\left(\sum_j w_j|j_0(k_i r)\delta_{ji} + T_{ji}(\sqrt{s})\widetilde{G}_j(r;s)|^2 - j_0^2(k_i r)\right), \quad (4)$$

where w_j is the weight of the observed channel j; $j_\nu(k_i r)$ is the spherical Bessel function; $E=\sqrt{s}$ is the CM energy; $k_i = \lambda^{1/2}(s, m_{1i}^2, m_{2i}^2)/(2\sqrt{s})$

is the relative momentum of the channel i, with λ being the Källen function and m_{1i}, m_{2i} the masses of the mesons in channel i; T_{ji} are the elements of the scattering matrix for the meson–baryon interactions; and the $\widetilde{G}_j(r;s)$ function is defined as

$$\widetilde{G}_j(r;s) = \int_{|\vec{q}|<q_{max}} \frac{d^3q}{(2\pi)^3} \frac{\omega_1^{(j)} + \omega_2^{(j)}}{2\omega_1^{(j)}\omega_2^{(j)}} \frac{j_0(qr)}{s - \left(\omega_1^{(j)} + \omega_2^{(j)}\right)^2 + i\varepsilon}, \tag{5}$$

with $\omega_a^{(j)} \equiv \omega_a^{(j)}(q) = \sqrt{q^2 + m_a^2}$ being the energy of the particle a in the channel j, and q_{max} being a sharp cutoff momentum introduced to regularize the $r \to 0$ behavior. The value of q_{max} is chosen to be $q_{max} =$ 700 MeV.

As discussed in the previous section, the ϕN system is described by the spin states 1/2 and 3/2. Therefore, each spin contribution should be weighted by the spin degeneracy, and the total ϕN CF is given by

$$C_{\phi N}(k) = \frac{1}{3} C_{\phi N}^{\left(\frac{1}{2}\right)}(k) + \frac{2}{3} C_{\phi N}^{\left(\frac{3}{2}\right)}(k), \tag{6}$$

where $C_{\phi N}^{(S)}(k)$ is estimated from Eq. (4) making use of the T-matrices determined in the corresponding spin s configuration.

Another important ingredient to be considered is the r-dependence of the source function. We employ the same parametrization adopted by the ALICE Collaboration in Ref. [1]. It is based on a static Gaussian profile normalized to unity, i.e.,

$$S_{12}(\vec{r}) = \frac{1}{(4\pi)^{\frac{3}{2}} R^3} \exp\left(-\frac{r^2}{4R^2}\right). \tag{7}$$

The source size parameter R in the present work is fixed at the central value used in Ref. [1]: $R = 1.08$ fm. A discussion on using other types of source functions can be found in Refs. [37,27].

The last elements to be remarked are the weights w_j's in Eq. (4). A common choice in the literature is $w_j = 1$ (see, e.g., the previous works [32–35] and references therein), which means the same final yield for all the observed channels. However, we know that the multiplicity of a two-particle channel is related to the number of its constituting primary particles, which depends on the collision conditions, such as the collision system (i.e., pp, pA, or AA), energy, and centrality interval considered. Thus, for the proper counting of the coupled channel correlations, it seems reasonable to consider different ω_js, as the primary yields generate pair multiplicities with very distinct magnitudes. In this regard, we benefit from the procedure reported in Ref. [5], where each contribution associated with the j-th transition has been weighted considering the data-driven method used in Ref. [38]. Accordingly, a given w_j is related to the multiplicity of the pairs yielded from primary particles generated in the collision. In turn, this amount of pairs has been obtained in Ref. [38] using the Thermal-Fist (TF) package [39,40], which is based on the statistical thermal model. The final number of pairs in the channel j is then the product between the primary yields of the particles in the considered pair, but taking into account pairs with relative momentum $k < 200$ MeV in the Monte Carlo simulations of the kinematic distributions. Thus, to make a reasonable comparison, the weights employed here in the calculations of the ϕN CF for the channel space in spin 3/2 are the same as those in Ref. [5], which have been calculated for the scenario of pp collisions at $\sqrt{s} = 13$ TeV. Concerning the remaining channels with spin 1/2, we have used the findings of Refs. [39,40], again using the same collision conditions. The w_j's are shown in Table 1, normalized with respect to the total production of ϕN pairs.

3. Results

We begin by showing in Fig. 2 the spin averaged correlation function obtained through Eq. (6), as a function of the CM relative momentum k. The calculation was done, for each spin case, using Eq. (4) with the weights listed in Table 1. For gaining a better understanding of this result, it is instructive to decompose it into its spin components. This is done in Fig. 3, where we plot the ϕN CF determined for the two spin channels 1/2 and 3/2. Clearly, the spin 3/2 amplitudes give a positive and much larger contribution to the full (spin-averaged) correlation function, while the corresponding spin 1/2 curve starts below unity and shows a much smaller momentum dependence. We note that this behavior is in qualitative agreement with what was found in Ref. [4]. In our approach, this agreement can only be achieved once spin-dependent interactions and all relevant coupled channels are taken into account (as will be shown below). Furthermore, we do find a strong attraction in the spin 3/2 case, in accordance with Ref. [2].

To understand this result further, we need to consider the spin 3/2 and 1/2 ϕN amplitudes in detail. First, we note that solving the Bethe-Salpeter equation in the approach followed in Refs. [6–8] involves regularizing a divergent loop function. This was done by following the

Table 1
Weights w_j's for the corresponding channels employed in the calculation of the coupled-channel ϕN CF shown in Eq. (6). The w_j's are normalized with respect to the total production of ϕN pairs, for the scenario of pp collisions at $\sqrt{s} = 13$ TeV.

j-th channel	$w_j^{\left(\frac{1}{2}\right)}$	$w_j^{\left(\frac{3}{2}\right)}$
πN	71	–
ηN	1	–
$K\Lambda$	5	–
$K\Sigma$	5	–
ρN	6.24	6.24
ωN	5.77	5.77
ϕN	1	1
$K^*\Lambda$	0.65	0.65
$K^*\Sigma$	0.42	0.42

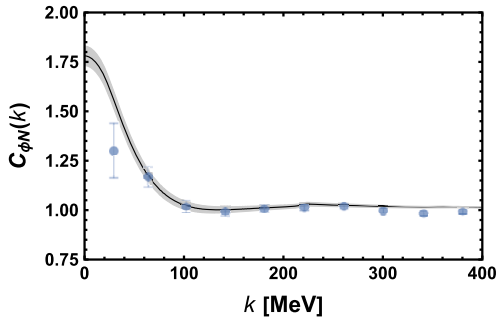

Fig. 2. Total coupled-channel ϕN CF defined in Eq. (6) as a function of the CM relative momentum k. The experimental points have been taken from Ref. [1]. As can be noticed, the results are shown in the form of a band which is associated with the uncertainty in the values of the weights given in Table 1. We consider the uncertainty to be of the order of ±10%.

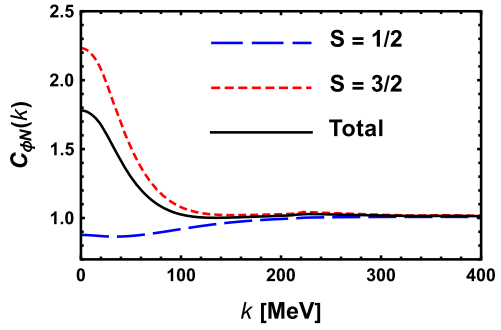

Fig. 3. The decomposition of the result shown in Fig. 2 into its $S = 1/2$ and $S = 3/2$ components.

Table 2
Values of the model parameters used to calculate spin-3/2 meson-baryon amplitudes.

Channel (i)	a_i (Set A)	a_i (Set B)
ρN	−2.0	−2.0
$\omega N N$	−2.0	−2.0
ϕN	−1.7	−2.0
$K^*\Lambda$	−2.1	−2.1
$K^*\Sigma$	−2.0	−2.0

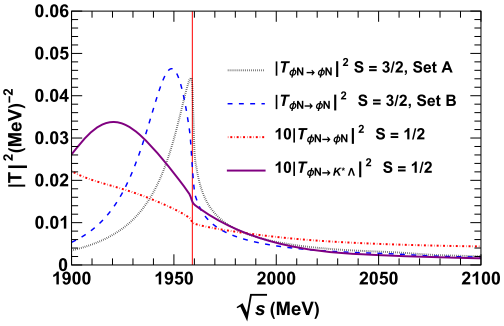

Fig. 4. A comparison of the amplitudes giving dominant contributions to the CF in the two spin configurations. We also show the effect of small changes made in the values of the parameters in the spin 3/2 case, which can turn the cusp near the ϕN threshold (shown as the dotted line) to a "bound" state (shown in the dashed line). The parameters are given in Table 2. Notice that a factor 10 is multiplied to the spin 1/2 amplitudes to facilitate a comparison with amplitudes in the spin 3/2 case.

dimensional regularization scheme, using a natural size [41] for the subtraction constants, $a_i = -2$, for each channel, i, in Ref. [6]. The study on the strangeness zero meson-baryon systems was further extended in Ref. [8] by including pseudoscalar-baryon systems in the formalism as coupled channels in the spin 1/2 configuration. In Ref. [8], the regularization parameters of the model were constrained to fit the experimental data on processes involving pseudoscalar-baryon systems. Hence, the subtraction constants for the spin 1/2 case can be considered to be fixed and should not be varied. In the spin 3/2 case, though, it is possible to vary slightly the parameters to study the uncertainties present in this case. With this in mind, we use two sets (A and B) of subtraction constants to calculate the spin 3/2 amplitudes. The respective values are listed in Table 2. As can be seen, both Set A and B are very close to the parameters used in Ref. [6]. We have used one of them, Set A, to prepare Figs. 2, 3, 5, and 6. As we will show, the two sets would lead to equivalent results. Set A corresponds to slightly reducing the attraction as compared to the work in Ref. [6], while Set B corresponds to slightly increasing the attraction. Although the T_{ji} matrices entering in Eq. (4) have been regularized by using subtraction constants, as done in Refs. [6–8], a unique sharp cut-off for all channels has been employed to regularize $\tilde{G}_j$ in Eq. (4). The latter method is more convenient in calculating the correlation function due to the presence of the Bessel function in $\tilde{G}_j$.

Let us now look at the obtained ϕN spin 1/2 and 3/2 amplitudes, shown together in Fig. 4, for comparison.

The spin 3/2 amplitudes show either a pronounced ϕN cusp (set A) or a bound state (set B). It is important to mention here that a strong cusp was present in the work of Ref. [6]. Although the spin 3/2 amplitudes are different for the two sets of parameters, especially below the ϕN threshold (vertical dashed line), the differences near (and above) the threshold are small, which implies that the correlation function is not sensitive to either choice of the parameters. Besides, it can be seen that the spin 1/2 amplitudes are much weaker around the ϕN threshold, which explains the small momentum dependence in Fig. 3. For the spin 1/2 case, it is however worth mentioning the important role of the $N^*(1895)$ in this region. To illustrate this, we in the same figure depict

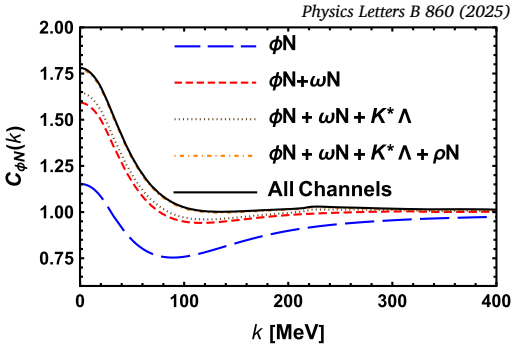

Fig. 5. Contribution of different channels to the ϕN CF defined in Eq. (6).

the $\phi N \to K^*\Lambda$ amplitude in which the existence of the $N^*(1895)$ is clearly visible. We must remark here that the mass of $N^*(1895)$ is not necessarily 1895 MeV, which is just an average mass value. It is useful to remark that a similar behavior of the CF, related to a shallow bound state, T_{cc} (and similar states) has been found in Refs. [32,33]. It is also important to recall that the behavior of the CF can very much depend on the channel of observation, coupled to the same state and to the size of the source function [42–48].

Comparing our results with those of Ref. [4], where an indication of the existence of a spin 1/2 ϕN bound state is found, we would like to mention that we are not sure if we can associate such a finding with the presence of $N^*(1895)$ in our amplitudes. It is a state that appears below the ϕ-N threshold, but it cannot be interpreted as a zero-width ϕN bound state in our formalism since it is coupled to several channels open for decay.

In this context, it is instructive to discuss the ϕN scattering length values obtained in the different spin cases. Before giving the explicit values, we should mention that the normalization used in our work to relate the scattering length with the t-matrix is

$$a^S_{\phi N} = -\frac{M_N}{4\pi\sqrt{s}} T^S_{\phi N}, \tag{8}$$

where M_N stands for the nucleon mass and the relation between the T-matrix and the amplitude V obtained from the effective Lagrangian is $T = V + VGT$. The scattering length value in the spin 1/2 case was already given in Ref. [8], but for the sake of completeness we here provide the values for both spin channels.

$$a^{S=1/2}_{\phi N} = -0.22 + i0.00 \text{ fm}, \tag{9}$$

$$a^{S=3/2,\text{set A}}_{\phi N} = -0.30 + i1.50 \text{ fm}, \tag{10}$$

$$a^{S=3/2,\text{set B}}_{\phi N} = -0.79 + i0.83 \text{ fm}. \tag{11}$$

Note that with the above conventions for a, T and V, negative values of the real part of a indicate either a repulsive interaction or the formation of a shallow bound state below the threshold. The reader may notice that the imaginary part of the spin 3/2 scattering length is bigger than the real part for parameter set A, while the real and imaginary parts are similar for parameter set B. Such a difference, and that in the overall values, corresponds to the change in the amplitude produced in the two cases. As seen in Fig. 4, a peak in the spin 3/2 amplitudes can be seen close to the ϕN threshold ($\sim$ 1959 MeV) for both sets of regularizing parameters. In both cases, a strong attraction arises from the coupled channel interactions. However, with set A, we find a strong cusp at the ϕN threshold, while with set B, a quasi-bound state appears in the complex energy plane. Since the state found in set B is below the ϕN threshold, when compared to the strong cusp obtained in set A, there is less phase space available for its decay to open channels, resulting in a smaller imaginary part of the ϕN t-matrix, which is related to the phase space via the implementation of unitarity in coupled channels. In view of Eq. (8), such a reduction of the imaginary part of the t-matrix produces a smaller imaginary part for the corresponding scattering length. It might

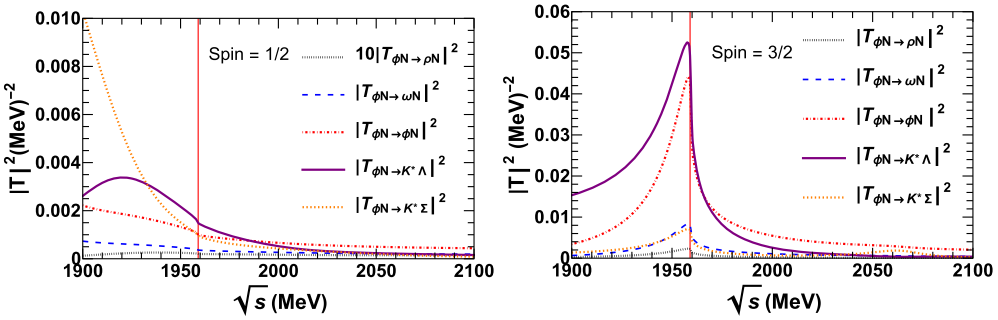

Fig. 6. This figure shows a comparison of the different amplitudes which are contributing to the CF in the spin 1/2 (left panel) and spin 3/2 (right panel) case. It can be seen that the dominant contribution comes from the ϕN and $K^*\Lambda$ channels.

also be useful to cite here the scattering length values for the $\bar{K}N$ system, which is related to the formation of the $\Lambda(1405)$. In Ref. [13], we find the scattering length for the isoscalar case where the real and the imaginary parts are of the same order. In the same work, we find that the imaginary part of the isovector scattering length is much bigger than its real part, and in this case, we find the dynamical generation of $\Sigma(1400)$. Our results are in good agreement with other studies (a list is available in the review presented in Ref. [49]). A similar feature has also been found for the ρN scattering length in Ref. [8].

Further, for the parameter set A, we get a spin averaged scattering length of $-0.22+i1.50$ fm, while for set B, we get $-0.72+i0.83$ fm. The absolute value of our results, which is about 1 fm, compares well with the one obtained through a Lednický–Lyuboshits fit made to the data on the spin-averaged ϕN correlation function [1]. The absolute value of the spin 3/2 scattering length found in our work also agrees well with that determined by lattice QCD [2]. It is, however, important to mention that the real and imaginary parts of our results, individually, do not agree well with the complex value determined in Ref. [1] for the spin averaged scattering length. Further, a purely real value of the spin 3/2 scattering length is obtained in Ref. [2]. To understand these differences we recall that the experimental data available on the correlation function is spin averaged. On the other hand, here, we study each spin case separately and find that the interactions are quite different and intricate in each case. It should not be surprising that the spin-averaged data can be described by a different combination of amplitudes for each spin case. We recall that the complex value determined for the spin 1/2 ϕN scattering length by the fit made to the ALICE data [1] in Ref. [4] is $\left(-1.54^{+0.53+0.16}_{-0.53-0.09}+i0.00^{+0.35+0.16}_{-0.00}\right)$ fm, a result which also differs from our findings.

Another issue to be addressed here is the difference between the order of magnitude of these scattering lengths and those obtained from the photoproduction processes. The absolute values of around 1 fm discussed above disagree by two orders of magnitude with the phenomenologically determined value for the $p\phi$ scattering length of 0.064 ± 0.010 fm in Ref. [3] using the total cross section data for the reaction $\gamma p\to\phi p$ from the CLAS Collaboration [50]. Furthermore, the values of the scattering lengths determined using recent LEPS data for $\gamma d\to\phi d\to K^+K^-d$ in Refs. [51–53], seem to be more in line with the values of Ref. [3]. In such a situation, it is important to understand if the interaction of a photon, reasoning in terms of vector meson dominance, through a $\bar{s}s$ pair, which eventually hadronizes as a ϕ meson, with the nucleon, could be different to the on-shell ϕN interactions. One has to also recall that there are subtleties involved in the determination of the scattering length from the correlation function as well, besides those mentioned in the previous paragraph. For example, the source radius depends on the multiplicity of a particular event. Some details on the determination of the size of the radius for average $\pi-\pi$ Bose-Einstein correlations are discussed in Refs. [54,55]. Additionally, initial correlations between protons and ϕ mesons are assumed to be negligible inside of the source radius of 1 fm. In any case, it is important to see if our model can provide a description for the discrepancy of the scattering length values coming from the photoproduction processes and those coming from the data on the correlation function [1] and lattice QCD [2]. Such a study should be done as a next step to this work.

Going back to the discussions of our results, we now consider the contributions of the most significant channels to the obtained correlation function. The corresponding decomposition for the spin averaged case is shown in Fig. 5.

It can be seen that the contributions from multiple channels have important contributions, the most important ones being ϕN and ωN. The corresponding amplitudes are shown in Fig. 6.

One can see that ϕN and $K^*\Lambda$ couple strongly in the spin 3/2 case to produce a cusp (or almost a bound state-like) structure near the ϕN threshold. In the case of spin 1/2, we have the presence of $N^*(1895)$, which was shown to have a two-pole nature in Ref. [8], with values $1801-i96$ MeV and $1912-i54$ MeV. As different channels have different couplings to the two poles, different structures appear in the amplitudes on the real axis.

4. Conclusions

In this work, we have calculated the correlation functions for the different spin configurations of the ϕN channel, taking into account spin-dependent vector-baryon interactions derived from an effective theory approach based on hidden local symmetry and coupled channel effects. We find that the presence of a strong attraction near the ϕN threshold in the spin 3/2 channel gives rise to a CF larger than 1 for small relative momentum. On the other hand, the spin 1/2 CF exhibits the opposite behavior, which we relate to the presence of the $N^*(1895)$ resonance in the scattering amplitudes. When combining the two spin channels to a spin-averaged quantity, we find reasonable agreement with the data reported by the ALICE Collaboration [1], which is achieved without any parameter fitting, but is rather a natural outcome of the model. We find that coupled channel effects are crucial in determining the CF. Furthermore, the weights ω_j for the different channels contributing to the CF are also a critical input necessary to reach a good agreement with the experimental data.

Declaration of competing interest

The authors declare the following financial interests/personal relationships which may be considered as potential competing interests: Alberto Martínez Torres reports financial support was provided by National Council for Scientific and Technological Development, Grant No. 304510/2023-8. Kanchan Khemchandani reports financial support was provided by National Council for Scientific and Technological Development, Grant No. 407437/2023-1 and No. 306461/2023-4. Luciano Abreu reports financial support was provided by National Council for Scientific and Technological Development, Grant No. 309950/2020-1,

400215/2022-5, 200567/2022-5, 464898/2014-5. Philipp Gubler reports financial support was provided by Coordination of Higher Education Personnel Improvement, Grant No. 001. Alberto Martinez Torres reports financial support was provided by State of São Paulo Research Foundation, Grant No. 2023/01182-7. Kanchan Khemchandani reports financial support was provided by State of São Paulo Research Foundation, Grant No. 2022/08347-9. Atsushi Hosaka reports financial support was provided by Japan Society for the Promotion of Science, Grant No. JP22H00122. If there are other authors, they declare that they have no known competing financial interests or personal relationships that could have appeared to influence the work reported in this paper.

Acknowledgements

This study was financed in part by the Coordenação de Aperfeiçoamento de Pessoal de Nível Superior – Brasil (CAPES) – Finance Code 001. The partial support from other Brazilian agencies is also gratefully acknowledged. We thank CNPq (L.M.A.: Grant No. 309950/2020-1, 400215/2022-5, 200567/2022-5; K.P.K: Grants No. 407437/ 2023-1 and No. 306461/2023-4; A.M.T: Grant No. 304510/2023-8), FAPESP (K.P.K.: Grant Number 2022/08347-9; A. M. T.: Grant number 2023/01182-7); and CNPq/FAPERJ under the Project INCT-Física Nuclear e Aplicações (Contract No. 464898/2014-5). A.H. is supported by the Grant-in-Aid for Scientific Research (A) (JSPS KAKENHI Grant Number JP22H00122).

Data availability

This is a theoretical work and the results are shown as plots in the manuscript.

References

[1] S. Acharya, et al., Experimental evidence for an attractive p-ϕ interaction, Phys. Rev. Lett. 127 (17) (2021) 172301, https://doi.org/10.1103/PhysRevLett.127.172301, arXiv:2105.05578.

[2] Y. Lyu, T. Doi, T. Hatsuda, Y. Ikeda, J. Meng, K. Sasaki, T. Sugiura, Attractive N-ϕ interaction and two-pion tail from lattice QCD near physical point, Phys. Rev. D 106 (7) (2022) 074507, https://doi.org/10.1103/PhysRevD.106.074507, arXiv:2205.10544.

[3] I.I. Strakovsky, L. Pentchev, A. Titov, Comparative analysis of ωp, ϕp, and $J/\psi p$ scattering lengths from A2, CLAS, and GlueX threshold measurements, Phys. Rev. C 101 (4) (2020) 045201, https://doi.org/10.1103/PhysRevC.101.045201, arXiv:2001.08851.

[4] E. Chizzali, Y. Kamiya, R. Del Grande, T. Doi, L. Fabbietti, T. Hatsuda, Y. Lyu, Indication of a p–ϕ bound state from a correlation function analysis, Phys. Lett. B 848 (2024) 138358, https://doi.org/10.1016/j.physletb.2023.138358, arXiv:2212.12690.

[5] A. Feijoo, M. Korwieser, L. Fabbietti, Relevance of the coupled channels in the ϕp and ρ^0p correlation functions (7 2024), arXiv:2407.01128.

[6] K.P. Khemchandani, H. Kaneko, H. Nagahiro, A. Hosaka, Vector meson-Baryon dynamics and generation of resonances, Phys. Rev. D 83 (2011) 114041, https://doi.org/10.1103/PhysRevD.83.114041, arXiv:1104.0307.

[7] K.P. Khemchandani, A. Martinez Torres, H. Kaneko, H. Nagahiro, A. Hosaka, Coupling vector and pseudoscalar mesons to study baryon resonances, Phys. Rev. D 84 (2011) 094018, https://doi.org/10.1103/PhysRevD.84.094018, arXiv:1107.0574.

[8] K.P. Khemchandani, A. Martinez Torres, H. Nagahiro, A. Hosaka, Role of vector and pseudoscalar mesons in understanding $1/2^- N^*$ and Δ resonances, Phys. Rev. D 88 (11) (2013) 114016, https://doi.org/10.1103/PhysRevD.88.114016, arXiv:1307.8420.

[9] K.P. Khemchandani, A. Martinez Torres, H. Nagahiro, A. Hosaka, Negative parity Λ and Σ resonances coupled to pseudoscalar and vector mesons, Phys. Rev. D 85 (2012) 114020, https://doi.org/10.1103/PhysRevD.85.114020, arXiv:1203.6711.

[10] K.P. Khemchandani, A. Martínez Torres, A. Hosaka, H. Nagahiro, F.S. Navarra, M. Nielsen, Why $\Xi(1690)$ and $\Xi(2120)$ are so narrow?, Phys. Rev. D 97 (3) (2018) 034005, https://doi.org/10.1103/PhysRevD.97.034005, arXiv:1608.07086.

[11] K.P. Khemchandani, A. Martinez Torres, H. Nagahiro, A. Hosaka, Decay properties of $N^*(1895)$, Phys. Rev. D 103 (1) (2021) 016015, https://doi.org/10.1103/PhysRevD.103.016015, arXiv:2010.04584.

[12] S.-H. Kim, K.P. Khemchandani, A. Martinez Torres, S.-i. Nam, A. Hosaka, Photoproduction of Λ^* and Σ^* resonances with $J^P = 1/2^-$ off the proton, Phys. Rev. D 103 (11) (2021) 114017, https://doi.org/10.1103/PhysRevD.103.114017, arXiv:2101.08668.

[13] K.P. Khemchandani, A. Martínez Torres, J.A. Oller, Hyperon resonances coupled to pseudoscalar- and vector-baryon channels, Phys. Rev. C 100 (1) (2019) 015208, https://doi.org/10.1103/PhysRevC.100.015208, arXiv:1810.09990.

[14] T. Hatsuda, S.H. Lee, QCD sum rules for vector mesons in the nuclear medium, Phys. Rev. C 46 (1) (1992) R34, https://doi.org/10.1103/PhysRevC.46.R34.

[15] K. Aoki, et al., Experimental study of in-medium spectral change of vector mesons at j-PARC, Few-Body Syst. 64 (3) (2023) 63, https://doi.org/10.1007/s00601-023-01828-7.

[16] P. Gubler, K. Ohtani, Constraining the strangeness content of the nucleon by measuring the ϕ meson mass shift in nuclear matter, Phys. Rev. D 90 (9) (2014) 094002, https://doi.org/10.1103/PhysRevD.90.094002, arXiv:1404.7701.

[17] H. Gao, T.S.H. Lee, V. Marinov, Phi - N bound state, Phys. Rev. C 63 (2001) 022201, https://doi.org/10.1103/PhysRevC.63.022201, arXiv:nucl-th/0010042.

[18] J.J. Cobos-Martínez, K. Tsushima, G. Krein, A.W. Thomas, Φ-meson–nucleus bound states, Phys. Rev. C 96 (3) (2017) 035201, https://doi.org/10.1103/PhysRevC.96.035201, arXiv:1705.06653.

[19] B.-X. Sun, Y.-Y. Fan, Q.-Q. Cao, The ϕ p bound state in the unitary coupled-channel approximation, Commun. Theor. Phys. 75 (5) (2023) 055301, https://doi.org/10.1088/1572-9494/acc31d, arXiv:2206.02961.

[20] A. Kuros, R. Maj, S. Mrowczynski, ϕ-p bound state and completeness of quantum states, vol. 8, arXiv:2408.11941, 2024.

[21] I. Filikhin, R.Y. Kezerashvili, B. Vlahovic, Possible Hϕ3 hypernucleus with the HAL QCD interaction, Phys. Rev. D 110 (3) (2024) L031502, https://doi.org/10.1103/PhysRevD.110.L031502, arXiv:2407.12190.

[22] I. Filikhin, R.Y. Kezerashvili, B. Vlahovic, Bound states of ${}^{9}_{\phi}$Be and ${}^{6}_{\phi\phi}$He with $\phi+\alpha+\alpha$ and $\phi+\phi+\alpha$ cluster models (8 2024), arXiv:2408.13415.

[23] R. Muto, et al., Evidence for in-medium modification of the phi meson at normal nuclear density, Phys. Rev. Lett. 98 (2007) 042501, https://doi.org/10.1103/PhysRevLett.98.042501, arXiv:nucl-ex/0511019.

[24] P. Gubler, M. Ichikawa, T. Song, E. Bratkovskaya, Production and in-medium modification of ϕ mesons in proton-nucleus reactions from a transport approach (8 2024) arXiv:2408.15364.

[25] E.Y. Paryev, Testing the ϕ-nuclear potential in pion-induced ϕ meson production on nuclei near threshold, Nucl. Phys. A 1032 (2023) 122624, https://doi.org/10.1016/j.nuclphysa.2023.122624, arXiv:2212.13778.

[26] H. Sako, et al., P88: Study of in-Medium Modification of ϕ Mesons Inside the Nucleus with $\phi \to k^+k^-$ Measurement with the e16 Spectrometer, Proposal for the 32nd J-PARC PAC Meeting, 2022.

[27] M.A. Lisa, S. Pratt, R. Soltz, U. Wiedemann, Femtoscopy in relativistic heavy ion collisions, Annu. Rev. Nucl. Part. Sci. 55 (2005) 357–402, https://doi.org/10.1146/annurev.nucl.55.090704.151533, arXiv:nucl-ex/0505014.

[28] S.E. Koonin, Proton pictures of high-energy nuclear collisions, Phys. Lett. B 70 (1977) 43–47, https://doi.org/10.1016/0370-2693(77)90340-9.

[29] S. Pratt, Pion interferometry of Quark-Gluon plasma, Phys. Rev. D 33 (1986) 1314–1327, https://doi.org/10.1103/PhysRevD.33.1314.

[30] R. Lednicky, V.L. Lyuboshits, Final state interaction effect on pairing correlations between particles with small relative momenta, Yad. Fiz. 35 (1981) 1316–1330.

[31] R. Lednicky, V.V. Lyuboshits, V.L. Lyuboshits, Phys. At. Nucl. 61 (1998) 2950.

[32] I. Vidana, A. Feijoo, M. Albaladejo, J. Nieves, E. Oset, Femtoscopic correlation function for the Tcc(3875)+ state, Phys. Lett. B 846 (2023) 138201, https://doi.org/10.1016/j.physletb.2023.138201, arXiv:2303.06079.

[33] A. Feijoo, L.R. Dai, L.M. Abreu, E. Oset, Correlation function for the T_{bb} state: determination of the binding, scattering lengths, effective ranges and molecular probabilities (9 2023), arXiv:2309.00444.

[34] M. Albaladejo, J. Nieves, E. Ruiz-Arriola, Femtoscopic signatures of the lightest S-wave scalar open-charm mesons, Phys. Rev. D 108 (1) (2023) 014020, https://doi.org/10.1103/PhysRevD.108.014020, arXiv:2304.03107.

[35] K.P. Khemchandani, L.M. Abreu, A. Martinez Torres, F.S. Navarra, Can a femtoscopic correlation function shed light on the nature of the lightest charm axial mesons?, Phys. Rev. D 110 (3) (2024) 036008, https://doi.org/10.1103/PhysRevD.110.036008, arXiv:2312.11811.

[36] M.-Z. Liu, Y.-W. Pan, Z.-W. Liu, T.-W. Wu, J.-X. Lu, L.-S. Geng, Three ways to decipher the nature of exotic hadrons: multiplets, three-body hadronic molecules and correlation functions (4 2024), arXiv:2404.06399.

[37] K. Kuroki, T. Hirano, p-ϕ interaction from femtoscopy using a dynamical model international workshop on J-PARC hadron physics 2024 (J-PARC Hadron 2024) 2024.

[38] S. Acharya, et al., Constraining the $\overline{\text{K}}$N coupled channel dynamics using femtoscopic correlations at the LHC, Eur. Phys. J. C 83 (4) (2023) 340, https://doi.org/10.1140/epjc/s10052-023-11476-0, arXiv:2205.15176.

[39] V. Vovchenko, B. Dönigus, H. Stoecker, Canonical statistical model analysis of p-p, p -Pb, and Pb-Pb collisions at energies available at the CERN large hadron collider, Phys. Rev. C 100 (5) (2019) 054906, https://doi.org/10.1103/PhysRevC.100.054906, arXiv:1906.03145.

[40] V. Vovchenko, H. Stoecker, Thermal-FIST: a package for heavy-ion collisions and hadronic equation of state, Comput. Phys. Commun. 244 (2019) 295–310, https://doi.org/10.1016/j.cpc.2019.06.024, arXiv:1901.05249.

[41] T. Hyodo, D. Jido, A. Hosaka, Origin of the resonances in the chiral unitary approach, Phys. Rev. C 78 (2008) 025203, https://doi.org/10.1103/PhysRevC.78.025203, arXiv:0803.2550.

[42] L. Fabbietti, V. Mantovani Sarti, O. Vazquez, Doce, study of the strong interaction among hadrons with correlations at the LHC, Annu. Rev. Nucl. Part. Sci.

71 (2021) 377–402, https://doi.org/10.1146/annurev-nucl-102419-034438, arXiv:2012.09806.

[43] R. Molina, C.-W. Xiao, W.-H. Liang, E. Oset, Correlation functions for the N*(1535) and the inverse problem, Phys. Rev. D 109 (5) (2024) 054002, https://doi.org/10.1103/PhysRevD.109.054002, arXiv:2310.12593.

[44] V.M. Sarti, A. Feijoo, I. Vidaña, A. Ramos, F. Giacosa, T. Hyodo, Y. Kamiya, Constraining the low-energy S = -2 meson-baryon interaction with two-particle correlations, Phys. Rev. D 110 (1) (2024) L011505, https://doi.org/10.1103/PhysRevD.110.L011505, arXiv:2309.08756.

[45] Z.-W. Liu, K.-W. Li, L.-S. Geng, Strangeness S = −2 baryon-baryon interactions and femtoscopic correlation functions in covariant chiral effective field theory*, Chin. Phys. C 47 (2) (2023) 024108, https://doi.org/10.1088/1674-1137/ac988a, arXiv:2201.04997.

[46] Z.-W. Liu, J.-X. Lu, L.-S. Geng, Study of the DK interaction with femtoscopic correlation functions, Phys. Rev. D 107 (7) (2023) 074019, https://doi.org/10.1103/PhysRevD.107.074019, arXiv:2302.01046.

[47] Z.-W. Liu, J.-X. Lu, M.-Z. Liu, L.-S. Geng, Distinguishing the spins of Pc(4440) and Pc(4457) with femtoscopic correlation functions, Phys. Rev. D 108 (3) (2023) L031503, https://doi.org/10.1103/PhysRevD.108.L031503, arXiv:2305.19048.

[48] Z.-W. Liu, J.-X. Lu, M.-Z. Liu, L.-S. Geng, Femtoscopy can tell whether $Z_c(3900)$ and $Z_{cs}(3985)$ are resonances or virtual states (4 2024), arXiv:2404.18607.

[49] M. Mai, Review of the Λ (1405) a curious case of a strangeness resonance, Eur. Phys. J. Spec. Top. 230 (6) (2021) 1593–1607, https://doi.org/10.1140/epjs/s11734-021-00144-7, arXiv:2010.00056.

[50] B. Dey, C.A. Meyer, M. Bellis, M. Williams, Data analysis techniques, differential cross sections, and spin density matrix elements for the reaction $\gamma p \to \phi p$, Phys. Rev. C 89 (5) (2014) 055208, https://doi.org/10.1103/PhysRevC.89.055208, Addendum: Phys. Rev. C 90 (2014) 019901, arXiv:1403.2110.

[51] C. Han, W. Kou, R. Wang, X. Chen, Extraction of ωn, ωp, and ϕN scattering lengths from ω and ϕ differential photoproduction cross sections on a deuterium target, Phys. Rev. C 107 (1) (2023) 015204, https://doi.org/10.1103/PhysRevC.107.015204, arXiv:2210.11276.

[52] T. Mibe, et al., Diffractive phi-meson photoproduction on proton near threshold, Phys. Rev. Lett. 95 (2005) 182001, https://doi.org/10.1103/PhysRevLett.95.182001, arXiv:nucl-ex/0506015.

[53] W.C. Chang, et al., Forward coherent phi-meson photoproduction from deuterons near threshold, Phys. Lett. B 658 (2008) 209–215, https://doi.org/10.1016/j.physletb.2007.11.009, arXiv:nucl-ex/0703034.

[54] V.A. Schegelsky, M.G. Ryskin, Bose-Einstein correlation to measure the size of event of different types (6 2015), arXiv:1506.03718.

[55] V.A. Schegelsky, M.G. Ryskin, Multiparticle production: an old-fashioned view (4 2016), arXiv:1604.01189.